

ORIGINAL ARTICLE

Sexual divergence in microtubule function: the novel intranasal microtubule targeting SKIP normalizes axonal transport and enhances memory

N Amram^{1,4}, G Hacoheh-Kleiman^{1,4}, S Sragovich¹, A Malishkevich¹, J Katz¹, O Touloumi², R Lagoudaki², NC Grigoriadis², E Giladi¹, A Yehekel³, M Pasmanik-Chor³, Y Jouroukhin¹ and I Gozes¹

Activity-dependent neuroprotective protein (ADNP), essential for brain formation, is a frequent autism spectrum disorder (ASD)-mutated gene. ADNP associates with microtubule end-binding proteins (EBs) through its SxIP motif, to regulate dendritic spine formation and brain plasticity. Here, we reveal SKIP, a novel four-amino-acid peptide representing an EB-binding site, as a replacement therapy in an outbred *Adnp*-deficient mouse model. We discovered, for the first time, axonal transport deficits in *Adnp*^{+/-} mice (measured by manganese-enhanced magnetic resonance imaging), with significant male–female differences. RNA sequencing evaluations showed major age, sex and genotype differences. Function enrichment and focus on major gene expression changes further implicated channel/transporter function and the cytoskeleton. In particular, a significant maturation change (1 month–five months) was observed in beta1 tubulin (*Tubb1*) mRNA, only in *Adnp*^{+/+} males, and sex-dependent increase in calcium channel mRNA (*Cacna1e*) in *Adnp*^{+/+} males compared with females. At the protein level, the *Adnp*^{+/-} mice exhibited impaired hippocampal expression of the calcium channel (voltage-dependent calcium channel, *Cacnb1*) as well as other key ASD-linked genes including the serotonin transporter (*Slc6a4*), and the autophagy regulator, *BECN1* (*Beclin1*), in a sex-dependent manner. Intranasal SKIP treatment normalized social memory in 8- to 9-month-old *Adnp*^{+/-}-treated mice to placebo-control levels, while protecting axonal transport and ameliorating changes in ASD-like gene expression. The control, all-D-amino analog D-SKIP, did not mimic SKIP activity. SKIP presents a novel prototype for potential ASD drug development, a prevalent unmet medical need.

Molecular Psychiatry (2016) **21**, 1467–1476; doi:10.1038/mp.2015.208; published online 19 January 2016

INTRODUCTION

Autism spectrum disorder (ASD) affects > 1.5% of children, with significantly higher prevalence in males and no cure to date.^{1,2} Activity-dependent neuroprotective protein (ADNP) is frequently mutated in cognitively deficient ASD cases.³ The human *ADNP* gene was mapped to chromosome 20q12-13.2 (ref. 4) and deletion in this chromosomal region resulted in mental retardation.⁵ ADNP, discovered in our laboratory,^{4,6} is essential for brain formation.⁷ ADNP interacts with heterochromatin protein alpha⁸ and constitutes a part of the SWI/SNF (mating type switching/sucrose nonfermenting) chromatin remodeling complex.⁹ Mouse *Adnp* regulates neurogenesis/embryogenesis through differential activation/silencing of > 400 genes.^{8,10} We have further shown a direct interaction of *Adnp* with (1) the polypyrimidine tract-binding protein-associated splicing factor,¹¹ with protein-associated splicing factor being a regulator of tau transcript splicing linked to frontotemporal dementia/tauopathy¹² and with tauopathy linked to autism;¹³ (2) eukaryotic initiation factor 4E^{14,15} that has been linked to autism;¹⁶ (3) microtubule (MT)-associated protein 1 light-chain 3 (*Map1lc3*), a key factor in autophagy induction, deregulated in neurodegenerative/neuropsychiatric diseases¹⁷ and autism;¹⁸ and (4) MT end-binding proteins (EBs)

through the SIP motif in it, which is also present in its neuroprotective snippet peptide, NAP (NAPVSIPQ).¹⁹ Together, these interactions point to the essential function for ADNP and to potential replacement therapies.

In contrast to the *Adnp*^{-/-} homozygous embryos, which present embryonic lethality, the *Adnp*^{+/-} mouse embryos undergo normal embryogenesis, albeit with slight developmental delays.⁷ Nonetheless, inbred *Adnp*^{+/-} mice exhibit cognitive deficits, significant increases in phosphorylated tau, tangle-like structures and age-dependent neurodegeneration as compared with *Adnp*^{+/+} mice.²⁰

The *Adnp*-derived NAP (NAPVSIPQ) was shown to mimic the neuroprotective activity of the parent protein. NAP protected against spatial memory impairments in the inbred *Adnp*^{+/-} mouse model.²⁰ Preclinical and clinical experiments demonstrated that intranasal administration of NAP to rat, dog or human results in measurable plasma levels of the drug and that the CNS is the pharmacodynamic compartment for NAP.²¹ No significant side effects were indicated.^{21,22} NAP also showed clinical efficacy in human studies enhancing daily activities and protecting brain matter metabolism/neuronal survival in schizophrenia patients and further protecting cognitive scores in amnesic mild

¹Lily and Avraham Gildor Chair for the Investigation of Growth Factors; Elton Laboratory for Neuroendocrinology; Department of Human Molecular Genetics and Biochemistry, Sackler Faculty of Medicine, Sagol School of Neuroscience and Adams Super Center for Brain Studies, Tel Aviv University, Tel Aviv, Israel; ²Department of Neurology, Laboratory of Experimental Neurology, AHEPA University Hospital, Aristotle University of Thessaloniki, Thessaloniki, Greece and ³Bioinformatics Unit, George S. Wise Faculty of Life Sciences, Tel Aviv University, Tel Aviv, Israel. Correspondence: Professor I Gozes, Lily and Avraham Gildor Chair for the Investigation of Growth Factors, Dr Diana and Zelman Elton (Elbaum) Laboratory for Molecular Neuroendocrinology, Sackler Faculty of Medicine, Tel Aviv University, Tel Aviv 69978, Israel.

E-mail: igozes@post.tau.ac.il

⁴These authors contributed equally to this work.

Received 14 February 2015; revised 17 November 2015; accepted 24 November 2015; published online 19 January 2016

cognitively impaired patients²³ at risk for Alzheimer's disease.²⁴ Although NAP (davunetide) provided protection in schizophrenia^{25,26} and mild cognitively impaired, it did not seem to offer protection in progressive supranuclear palsy patients,²⁷ possibly due to insufficient target engagement coupled to advanced, irreversible disease stage. To improve the efficacy of NAP, studies were launched to precisely delineate its mechanism of action, which was originally shown to protect MTs.²⁸ We identified the shared Adnp and NAP SIP motif as directly interacting with the MT EB proteins EB1 and EB3. Silencing of either EB1 or EB3 abolished NAP cell protection.¹⁹ Furthermore, silencing EB3 abolished NAP-enhancement of dendritic spine formation. By protecting the MTs, NAP protected the autophagy process,²⁹ and enhanced I ϵ 3/Adnp interaction.¹⁷

Several NAP (NAPVSIQ) analogs were designed, which included alterations of the EB1/EB3-interacting SxIP motif. Although NAPVSKIPIQ and Ac-NAPVSKIPIQ-NH₂ interacted with EB3 and mimicked NAP activities, NAPVSRIPQ and NAPVTRIPQ were inactive and NAPVSAIPQ as well as NAPVAAAQ failed to displace NAP-EB3 binding.¹⁹ Original studies suggested that a peptide length of 8–9 amino acids, including the SIP motif, is required for neuroprotection.^{30,31}

Now, we ask: (1) Is it possible to shorten NAP, to an active SxIP peptide? (2) Given the ADNP-MT connection, are MTs impaired in the Adnp^{+/-} mouse? (3) Are there additional consequences to Adnp deficiency in mice that could be ameliorated by SxIP treatment? We disclose here the four-amino-acid SKIP, an EB1/EB3-targeting drug candidate with an ideal brain penetration size of ~400 Da.³² SKIP ameliorated marked deficits associated with Adnp deficiency *in vivo*. Given the severe breeding difficulties in Adnp^{+/-} mice, we utilized an outbred mouse model (Adnp^{+/-} crossed with ICR), exhibiting autistic-like sexual dichotomy.¹⁵ We further discovered that even basic mechanism in neuronal function, including axonal transport and autophagy, exhibited sexual dimorphism. RNA sequencing (RNA-seq) analysis extended these findings and pointed to channel and transporter regulation as central for the activities of Adnp.

MATERIALS AND METHODS

In silico analysis

Initial complexes were modeled using structural alignment of PDB entries 3GJO (EB3 homodimer³³) and 3TQ7 (EB1-EB3 heterodimer³⁴), using Pymol, in order to create EB3 and EB1 homodimers bound to each peptide. The Rosetta FlexPepDock protocol for high-resolution docking of flexible peptides³⁵ was used to dock SKIP and NAPVSIQ to EB3. This protocol allows flexibility of receptor's side chains in close proximity to the peptide, as well as full flexibility of the peptide. Two hundred possible poses (conformations of peptides and positions in the receptor binding site) of each complex were created, and the best scoring poses are presented below (Figures 1a and b).

Affinity chromatography

The SulfoLink Immobilization Kit for Peptides (44999, Thermo Scientific, Rockford, IL, USA) was used to determine whether there is a competition between SKIP and NAP for the same binding site of recombinant EB3.¹⁹

Nuclear magnetic resonance (NMR) spectroscopy

NMR was carried out in the service unit of Tel Aviv University as detailed in Figure 1.

Rat pheochromocytoma cells

Rat pheochromocytoma cell (PC12, ATCC, Bethesda, MD, USA) was grown and submitted to zinc intoxication as before.¹⁹

Animals

All procedures involving animals have been approved by the Animal Care and Use Committee of Tel Aviv University and the Israeli Ministry of Health.

Adnp^{+/-} mice on a mixed C57BL and 129/SvJ background, a model for cognitive impairments,⁷ were housed in a 12-h light/12-h dark cycle facility, and free access to rodent chow and water was available. The procedure to generate Adnp^{+/-} animals was previously described^{17,20} and genotyping was performed by Transnetyx (Memphis, TN, USA). An ICR outbred mouse line, which allows for continuous breeding and excellent progeny, was used.¹⁵

Peptide synthesis and SKIP treatment

Peptides synthesized using conventional methods³⁶ were purchased from Hay Laboratories (Rehovot, Israel). SKIP treatment included twice daily intranasal administrations to 6-month-old male mice (2 μ g/5 μ l per mouse per dose). The peptide was dissolved in a vehicle solution³⁷ (Supplementary File). After 1 month, SKIP was applied 2 h before the behavioral tests (below). Unless otherwise stated, four groups from each sex (males and females) were tested. Animals were numbered and randomly assigned to the different groups. Group size was determined by previous experience with the Adnp/ICR outbred line: Adnp^{+/+}/DD ($n=16$); Adnp^{+/+}/SKIP ($n=18$); Adnp^{+/-}/DD ($n=14$); Adnp^{+/-}/SKIP ($n=16$).

A control peptide, all D-amino acid SKIP, D-SKIP was applied as above to males only, Adnp^{+/+} ($n=8$), Adnp^{+/-} ($n=12$).

Manganese-enhanced magnetic resonance imaging (MEMRI) estimation of axonal transport rate

MEMRI was conducted as described.³⁸ Adnp^{+/+} and Adnp^{+/-} mice (5 months of age at the time of testing, $n=3-6$ /group) were anesthetized by inhalation of 1–1.5% isoflurane and intranasally administered with 4 μ l of 0.5 M MnCl₂ (Sigma) dissolved in PBS in each nostril. Selected groups of Adnp^{+/-} mice were intraperitoneally injected with 10 μ g SKIP/0.3 ml saline. The rate of axonal transport was evaluated by serial T1-weighted images (Supplementary File).

Next-generation sequencing (RNA-seq) and analysis

RNA-seq comparisons between males and females, genotype (Adnp^{+/+}/Adnp^{+/-}) and age dependence, included 1-month-old mice ($n=12$) and 5-month-old mice ($n=11$), three per group, with one Adnp^{+/-} group including two males. Selected results were verified by quantitative real-time PCR. Detailed methodology is given in the Supplementary Tables 1 and 2. Data were submitted to GEO, accession number GSE72664.

Immunohistochemistry

Nine-month-old mice were perfused transcardially under deep anesthesia with 4% paraformaldehyde (PFA) in 0.1 M PBS, PH 7.4 and their brains were removed, post-fixed in the same fixative and embedded in paraffin. Histological staining and immunohistochemistry were performed on 6 μ m serial brain sections (Supplementary File). The evaluation was performed on the area of the hippocampus (CA1) and the prefrontal cortex. Supplementary Figure 1 shows a lower magnification pointing out the precise choice of tissue for further analysis.

Social recognition and social memory test

This behavioral paradigm was described before.¹⁵ Mice were 8-month-old at the time of testing. The social approach task was adapted from a previously reported procedure³⁹ (Supplementary File). The data were analyzed using the following formula: $D2 = (b-a)/(b+a)$, when 'a' designated the time of exploration of the familiar mouse and 'b' designated the time of exploration of the novel mouse. The formula evaluates the discrimination capacity of the mice between the novel mouse and the familiar mouse.⁴⁰

Odor habituation/dishabituation test

This test, based on previous observations,^{41–43} was performed as described in our previous study¹⁵ (Supplementary File).

Statistical analysis

Results are described as means \pm standard error of the mean (s.e.m.). Statistical details including the analysis of the RNA-seq data can be found in the Supplementary file and in the figure legends.

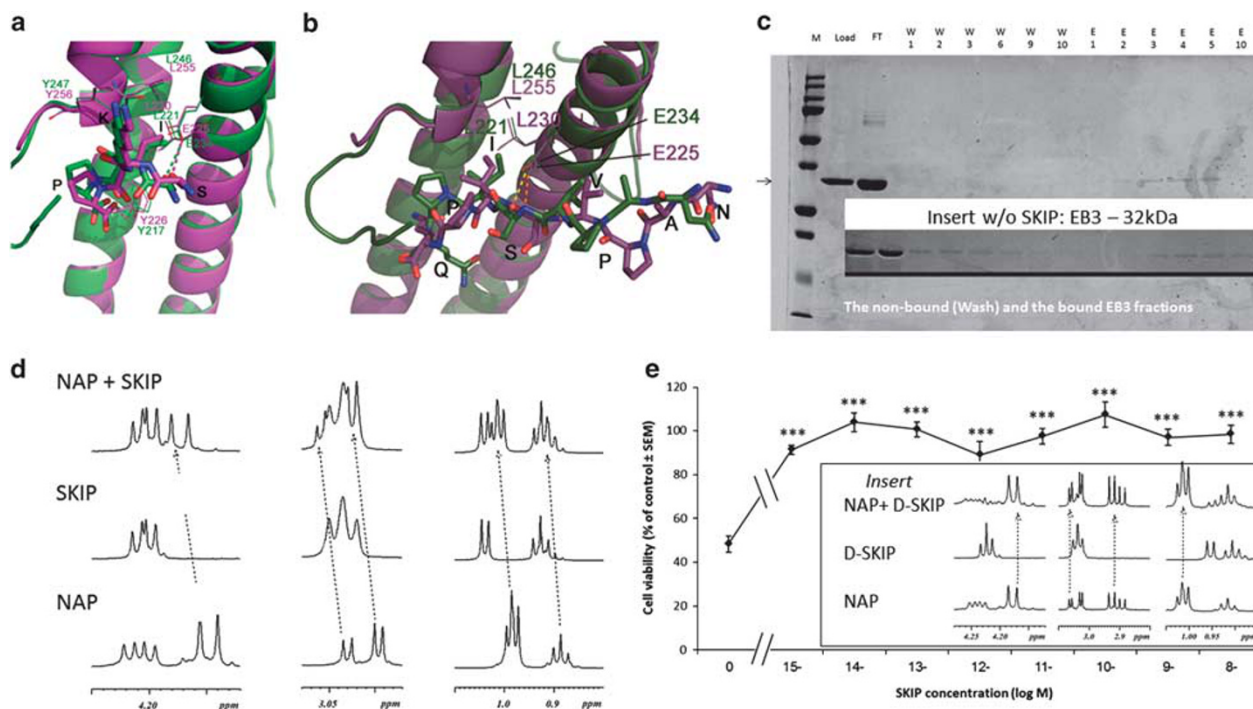


Figure 1. SKIP, an EB3-binding peptide *in silico*, binds to the activity-dependent neuroprotective protein-derived NAP (NAPVSIPQ), enhances NAP–EB3 interaction and protects PC12 cells against zinc intoxication. **(a)** Three-dimensional (3D) structures of EB1 homodimer (green) and EB3 homodimer (magenta) are shown as ribbons. Residues that are predicted to bind SKIP peptide are shown as lines. SKIP peptide is shown as sticks. A possible hydrogen bond between the peptide's serine side chain and receptor's glutamate is shown by dashed line. The figure was generated using Pymol. **(b)** 3D structures of EB1 homodimer (dark green) and EB3 homodimer (purple) are shown as ribbons. Residues that are predicted to bind NAPVSIPQ peptide are shown as lines. NAPVSIPQ peptide is shown as sticks. A possible hydrogen bond between the peptide's serine backbone and receptor's glutamate is shown by dashed line. The figure was generated using Pymol. Of note, the resolution of the EB1 and the EB3 crystal structures in the area that surrounds the proline of SxIP motif of NAP peptide does not allow the exact estimation of the binding site residues. **(c)** There is no competition between SKIP and (CKKKGGNAPVSIPQ) for the NAP-binding site of EB3. C-NAP (3 mg) was bound to the SulfoLink Column (containing coupling resin) according to the manufacturers' instruction. Subsequently, bovine serum albumin (3 mg) was loaded on the column to block nonspecific binding sites. Thereafter, recombinant EB3 (3 mg) together with SKIP (3 mg) were loaded on the resulting C-NAP-coupled SulfoLink column. To qualitatively monitor the binding efficiency of EB3, fractions from the following steps were collected: load, flow-through (FT), wash (W1–10), elution (E1–10) and then EB3 was identified using SDS-polyacrylamide gel (PAGE) electrophoresis, followed by Coomassie Brilliant Blue staining. The figure shows the Coomassie Blue-stained SDS-PAGE gel. Each lane represents a step in the procedure. EB3 was detected in the load and FT and in the NAP-binding EB3 fractions—elution fraction (E) and not in the wash-through fractions, contrasting previous data, where the column was performed without (w/o) SKIP and EB3 was found also in the column wash fractions (inset). **(d)** Interaction (nuclear magnetic resonance (NMR) experiments): Diffusion experiments were carried out in the service unit at Tel Aviv University on a 500-MHz Avance III Bruker (Karlsruhe, Germany) NMR spectrometer equipped with a pulsed gradient unit capable of producing magnetic field pulse gradients of $\sim 50 \text{ G cm}^{-1}$ in the z-direction. One-dimensional spectra analysis showed a shift in the spectra of the mixture of NAP and SKIP, compared with the individual spectra, indicating binding. Approximately 15% of the material was bound indicative of a binding constant of 30. In contrast, no shift was observed in D-SKIP+NAP mixture, indicating no direct binding. **(e)** Rat pheochromocytoma cells (PC12) were seeded on poly-D-lysine-coated 96-well tissue culture dishes at a concentration of 30 000 cells per well and allowed to adhere overnight. On the following day, cell growth medium was removed and replaced by either a fresh growth medium (control group) or ZnCl_2 ($400 \mu\text{M}$) either alone or in combination with different concentration of SKIP for 4 h. After 4 h, cell viability was analyzed by the MTS assay. Control = 100% viability. SKIP showed protection against zinc intoxication in concentrations of 10^{-15} M to 10^{-8} M (significantly higher viability compared with zinc alone). Data were normalized to % of control. The results are shown as mean \pm s.e.m. of three independent experiments, each performed in hexuplicate ($n = 16\text{--}18$). $***P < 0.001$ for the difference from untreated control. M, Marker.

RESULTS

SKIP, like NAP interacts with EB3 and provides protection against zinc intoxication

In silico analyses introduce here, for the first time, the four-amino-acid SKIP as an EB1/EB3-targeting drug candidate (Figure 1a), compared with NAP (Figure 1b). In comparison to the SxIP-containing peptide, which was crystallized with the EB1 homodimer,³³ SKIP is modeled to bind EB1 and EB3 using the same residues (Figure 1a). Serine is predicted to bind Glutamate 225 in EB3 and Glutamate 234 in EB1. Isoleucine (I) is predicted to point to the hydrophobic pocket, which includes Leucine (L) L246/L255 and L221/L230 in EB1/EB3, respectively. Lysine (Y) is

predicted to point away from the protein and Proline (P) is predicted to bind Y226/Y217 L230 in EB1/EB3, respectively. NAP (NAPVSIPQ) was modeled to bind EB1 and EB3 using the same residues as Serine (S) and Isoleucine (I) of SKIP. Although the resolution of the EB1 and the EB3 crystal structures in the area that surrounds the Proline of SxIP motif of NAP peptide did not allow the exact estimation of the binding site residues, unlike SKIP, the Serine in NAP was not bound using its side chain but its backbone (Figure 1b).⁴⁴

Interestingly, SKIP did not displace NAP (immobilized CKKKGGNAPVSIPQ)–recombinant EB3 interaction,¹⁹ but rather showed an increased interaction over the immobilized NAP–EB3 interaction (that is, the absence of EB3 elution in the column wash

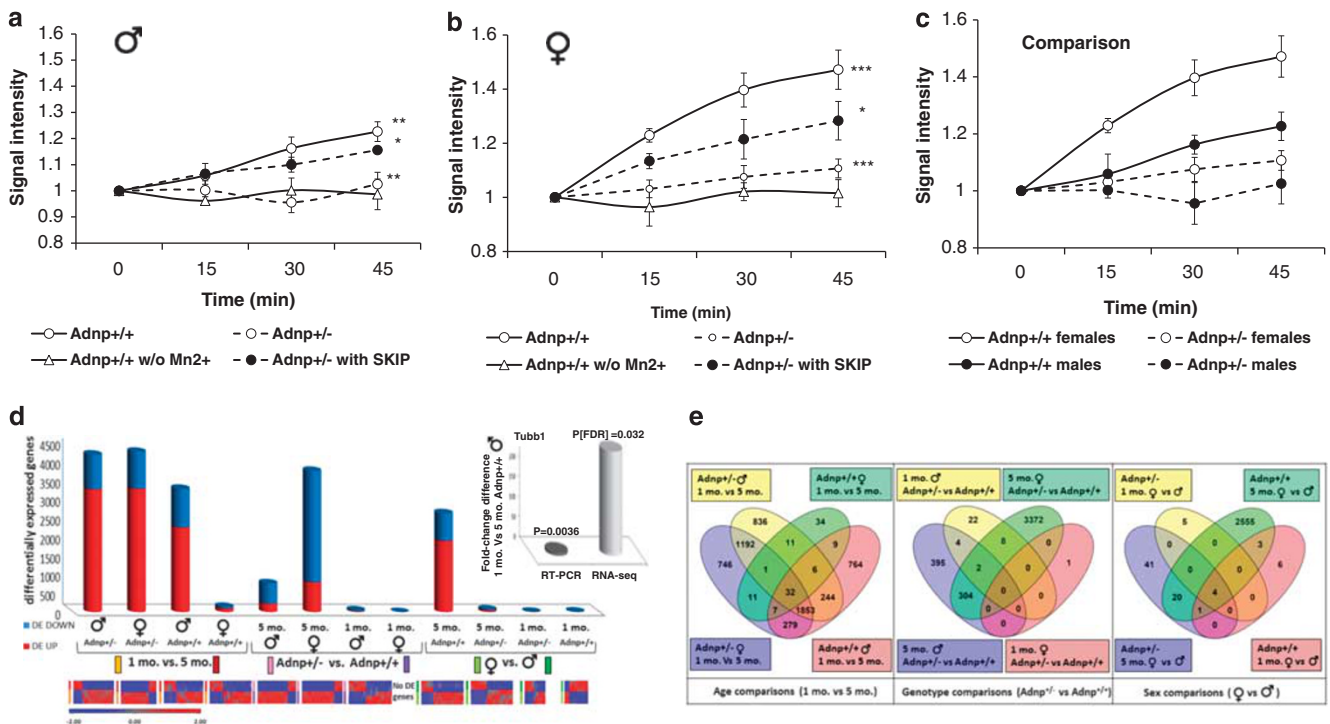


Figure 2. Manganese-enhanced magnetic resonance imaging estimation of axonal transport rates shows impairment in Adnp^{+/-} mice and repair by SKIP treatment, coupled to sex differences. **(a)** Signal intensity changes of T1-weighted images measured during ~45 min in Adnp^{+/-} male mice without (w/o) Mn2+ ($n=4$), or Adnp^{+/-}+Mn2+ ($n=6$), Adnp^{+/-}+Mn2+ ($n=6$), or SKIP-treated Adnp^{+/-}+Mn2+ ($n=5$). Repeated measure analysis of variance (ANOVA) followed by Fisher's LSD was used to analyze the data. Transport rate was significantly slower in the Adnp^{+/-} male mice compared with the Adnp^{+/-} group (mean difference of 0.116 ± 0.03 , $P < 0.01$, LSD). Sham-treated Adnp^{+/-} mice did not show increases of signal intensity ($P > 0.05$) and exhibited a significantly lower signal than the signal intensity observed in WT mice treated with manganese (mean difference of 0.124 ± 0.03 , $P < 0.01$, LSD). Adnp^{+/-} mice pretreatment with SKIP (10 μ g per 0.3 ml saline) resulted in significant increases in axonal transport (mean difference of 0.084 ± 0.03 , $P < 0.05$, LSD). * $P < 0.05$, ** $P < 0.01$. **(b)** Repeated measure ANOVA followed by Fisher's LSD revealed that the measured axonal transport rate was significantly slower in the Adnp^{+/-} female mice ($n=6$) compared with the Adnp^{+/-} group ($n=5$; mean difference of 0.221 ± 0.04 $P < 0.001$, LSD *Post Hoc* test). Sham-treated Adnp^{+/-} mice ($n=3$) did not show increases of signal intensity ($P > 0.05$) and exhibited a significantly lower signal than the signal intensity observed in Adnp^{+/-} mice treated with manganese ($n=5$; mean difference of 0.274 ± 0.05 , $P < 0.001$, LSD). SKIP treatment ($n=6$) significantly increased Adnp^{+/-} axonal transport (mean difference of 0.105 ± 0.04 , $P < 0.05$, LSD *post hoc* test). * $P < 0.05$, *** $P < 0.001$. **(c)** Overall comparison among four groups: male and female mice of Adnp^{+/-} and Adnp^{+/-} genotypes (male Adnp^{+/-} $n=6$, male Adnp^{+/-} $n=6$, female Adnp^{+/-} $n=3$, female Adnp^{+/-} $n=4$), using repeated measures ANOVA, found significant gender \times genotype interaction ($F(1,15)=9.26$, $P < 0.01$). Measured axonal transport rate was significantly slower in Adnp^{+/-} transgenic mice in comparison to the Adnp^{+/-} group (mean difference of 0.187 ± 0.023 , $F(1,15)=64.62$, $P < 0.001$) and in males in comparison to females (mean difference of 0.109 ± 0.023 , $F(1,15)=21.92$, $P < 0.001$). **(d)** RNA-seq analysis, differentially expressed genes (using cutoffs $P(\text{FDR}) < 0.05$ and fold-change difference = 2; y axis) were obtained for the various comparisons (x axis). Upregulated genes are colored red, downregulated genes are colored blue. The inset shows quantitative real-time validation of major changes in beta tubulin 1 expression (Tubb1) with higher levels of expression in 1-month-old Adnp^{+/-} males compared with 5-month-old (t-test). The inset below the x axis shows the heat-map for each condition (See Supplementary Figure 3 for more details. Mo=month, DE=differentially expressed.). **(e)** Venn graph of differentially expressed genes shows a comparison age, genotype and sex, indicating the number of common and unique genes.

fraction, Figure 1c, W1–10), in agreement with the original suggestion that binding of one SxIP residue enhances the interaction of another SxIP residue.³ Indeed, NMR analysis showed that the ADNP-derived NAP (NAPVSIPQ) interacted with SKIP (Figure 1d) and that the all D -amino-acid SKIP (control) did not (Figure 1e, inset). In a cell culture model of zinc intoxication, which has been shown before to affect the MT system,¹⁹ SKIP protected cell viability over a large range of concentrations (Figure 1e).

SKIP protects against axonal transport deficits inflicted by Adnp deficiency

To address the question if Adnp deficiency is associated with MT functional impairment, we have measured axonal transport, which depends on MT integrity. We used the MEMRI method.³⁸ Increased signal intensity in the lateral part of the olfactory nerve and glomerular layer, reflecting anterograde axonal transport of Mn2+,

was detected in 5-month-old Adnp^{+/-} male mice ~30–40 min after Mn2+ application. Signal intensity was significantly reduced in Adnp^{+/-} male mice reflecting impaired axonal transport of Mn2+. Contrarily, Adnp^{+/-} mice pretreated with SKIP revealed significant increases in signal intensity, reflecting axonal transport, up to the level of Adnp^{+/-} mice (Figure 2a). Similar results were found in female mice (Figure 2b). Surprisingly, comparison between males and females showed a significant overall difference, with faster axonal transport in females (Figure 2c).

Non-biased RNA-seq identifies key pathways

RNA-seq of total hippocampal gene expression followed by bioinformatics enrichment of modified networks was coupled to real-time PCR validation and immunohistochemistry (Figures 2d and e). Comparisons indicated 2583 differentially expressed genes between 5-month-old Adnp^{+/-} females and males. Adnp

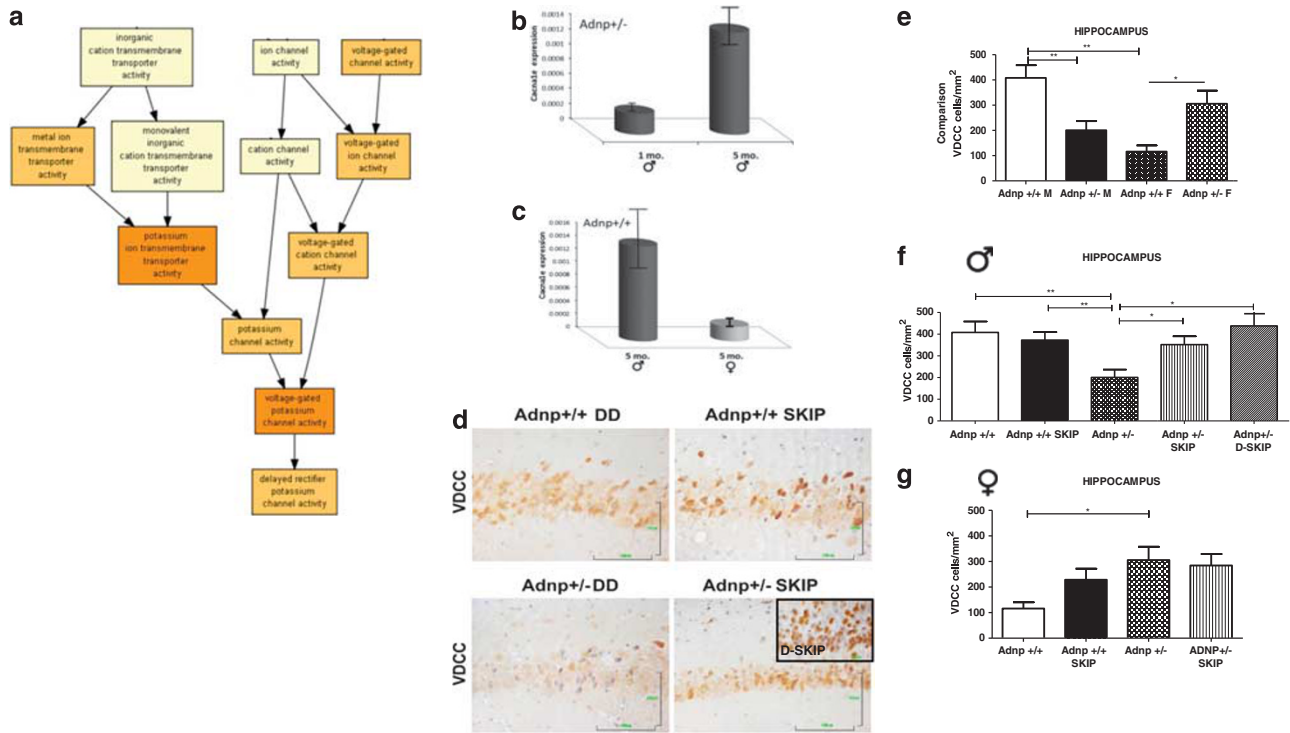


Figure 3. Adnp deficiency results in calcium channel changes characteristic to autism spectrum disorder and associated with sexual differences. **(a)** Molecular function enrichment analysis was performed on differentially expressed hippocampal genes of 5-month female Adnp^{+/-} compared with Adnp^{+/+} by GOrilla tool (Supplementary Figure 3). Enriched functions are shown in a graphic representation. Darker colors present higher enrichment. High enrichment was found for ion channels, including calcium channels and peaked ($P(\text{FDR}) = 2.52E-05$) with potassium ion transmembrane transporter activity function. **(b and c)** Representative calcium channel differences in gene expression were further studied by quantitative real-time PCR (Supplementary file; $P = 0.05$, t -test, mo = months). **(b)** Age differences in Adnp^{+/-} males. **(c)** Sex differences in 5-month-old Adnp^{+/+} mice. **(d-g)** Coronal tissue brain sections from 9-month-old mice ($n = 5$ mice/group) were studied in the hippocampus (CA1). Data analysis was performed using the GraphPad Prism 5.0 software. The normality was tested using the Shapiro-Wilk and Kolmogorov-Smirnov tests. Parametric data were analyzed using one-way analysis of variance (ANOVA) with Bonferroni's Multiple Comparison test. Bar graphs represent means (cells per mm²) ± s.e.m. **(d)** Representative immunohistochemical panels for the voltage-dependent calcium channel (VDCC; Cacnb1, males), bars = 100 μm. **(e)** Comparing Adnp^{+/-} males to females showed fourfold increased expression in VDCC in males. **(f)** Adnp^{+/-} male mice exhibited a reduced number of cells expressing VDCC (** $P < 0.01$), compared with Adnp^{+/+}. SKIP and D-SKIP treatment significantly increased VDCC levels in the hippocampus of Adnp^{+/-} male mice (* $P < 0.05$), although in the case of D-SKIP, the increase seemed apparently greater. **(g)** In contrast to males, Adnp^{+/-} female mice exhibited a threefold increase in VDCC expression compared with Adnp^{+/+}, which was not reduced by SKIP treatment.

haploinsufficiency in 5-month-old females resulted in 3686 differentially expressed genes (Figure 2e). Most robust age-dependent differences (1 and 5 months) were observed in Adnp^{+/-} mice (~4000 genes; Figure 2d). Heat maps verified the data and indicated multiple differences (Figure 2d and Supplementary Figure 2). Five out of eight derived enriched function maps (Supplementary Figure 3) culminated with ion transport. The Adnp-deficient genotype affected differently males and females at the age of 5 months, with males specifically showing changes in functional phosphoinositol and lipid binding. Furthermore, ribosome structure function changed age-dependently and a most striking male to female difference was in general receptor activity. Genes that showed the largest differences in expression (Supplementary Table 3) also indicated changes involving signaling, transcription and critical life-death pathways. Diseases associated included deafness and cancer. Developmental retardation (brain, heart, muscle and sex-related) were noticed in the Adnp-deficient mice, as well as potential deficits in the blood-brain barrier, food intake, circadian activity (sleep), all partially impacting ADNP-mutated children.^{3,4,5,46} At least 10% of the major gene changes were associated with calcium metabolism and an additional ≥ 10% of the changes were associated with the cytoskeleton, probably related to the observed differences in axonal transport. Although EBs (Mapre genes) and

tau (Mapt) did not change, looking at all the tubulin genes showed a 1- to 5-month significant decrease in tubulin beta 1 (Tubb1) expression in Adnp^{+/+} males (>350-fold) and the decrease was validated by real-time PCR (~10-fold, Figure 2d, inset).

Focusing on calcium and sex differences, a major genotype difference was observed in 5-month-old females (Figure 2d), including the voltage-dependent calcium channels (VDCCs; Figure 3a).

Cacna1e (CaV2.3), a VDCC gene implicated in dendritic spine formation,⁴⁷ showed most robust age- and sex-dependent differences in expression, as further studied by RT-PCR concentrating on exon 6 of the 50 exons of the gene (<http://www.ncbi.nlm.nih.gov/IEB/Research/Acembly/av.cgi?db=human&l=CACNA1E>; Figures 3b and c). Specifically, expression was increased at 5 months compared with 1 month of age and males showed increased hippocampal expression compared with females, at 5 months. Immunohistochemically, we showed a similar sex- and genotype-associated changes, with Adnp^{+/-} male mice exhibiting reduced number of cells expressing the VDCC protein (Cacnb1, hippocampus, $P < 0.01$, Figures 3d-f). SKIP treatment significantly increased VDCC levels in the Adnp^{+/-} male mice ($P < 0.05$; Figures 3d and f). This was mimicked by D-SKIP with an apparently greater increase. In females, which compared with males, showed

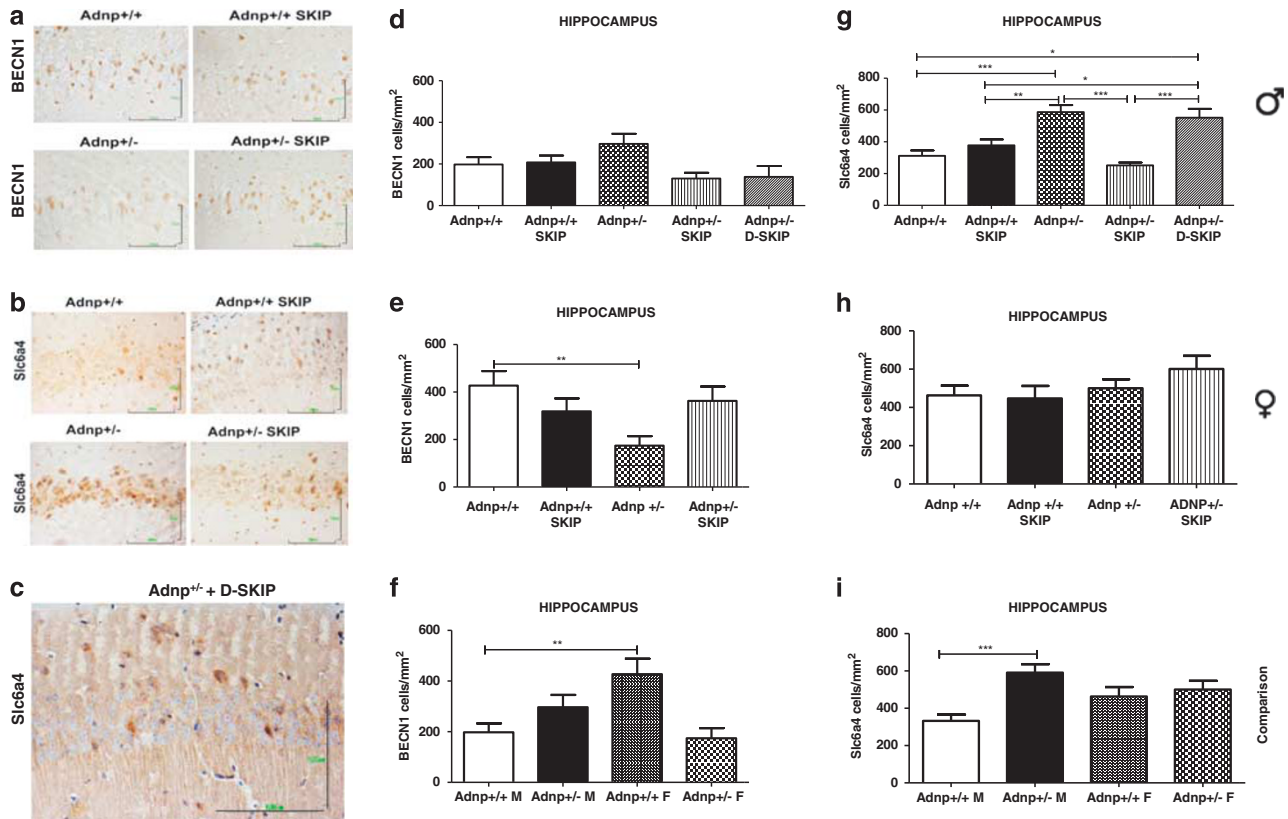


Figure 4. Adnp deficiency results in changes characteristic to autism spectrum disorder (ASD) and associated with sexual differences: amelioration by SKIP. Representative immunohistochemical panels (prepared as in Figure 3) are shown, bars = 100 μ m. (a) Female, hippocampus, CA1, BECN1; (b) Male, hippocampus, CA1, Slc6a4; (c) Male, hippocampus D-SKIP. (d) Males, (e) females, (f) comparisons: BECN1 (Beclin1), a significant twofold reduction in hippocampal BECN1 expression levels in the Adnp^{+/-} female mice, compared with Adnp^{+/+} (***P* < 0.01), SKIP treatment insignificantly increased BECN1 levels in the Adnp^{+/-} mice (e). Females showed twofold increased BECN1 hippocampal expression compared with males (f). (g) Males, (h) females, (i) comparisons: Slc6a4 (serotonin transporter), a significant twofold increase in hippocampal Slc6a4 expression levels in the Adnp^{+/-} male mice, compared with Adnp^{+/+} (***) (*P* < 0.001). SKIP treatment reduced Slc6a4 levels in the Adnp^{+/-} mice (***) (*P* < 0.001), whereas D-SKIP did not (g). No effect in females (h) and no difference between sexes with the same Adnp genotype were observed (i). **P* < 0.05.

decreased (fourfold) number of VDCC protein-expressing cells, Adnp haploinsufficiency resulted in a threefold increase in these cells, with no effect of SKIP treatment (Figures 3e and g).

As indicated above, cytoskeletal genes showed major changes, and as the cytoskeletal system and ADNP are linked to the autophagy pathway, we have also looked at BECN1 (Beclin1). BECN1 RNA-seq results at the gene level were negligible as verified by RT-PCR (not shown). However, Figures 4a and d–f show a significant decrease of BECN1 expression in females only with SKIP-treated Adnp^{+/-} showing similar results to Adnp^{+/+}. Interestingly, Adnp^{+/+} females expressed ~2-fold more hippocampal BECN1 cells than Adnp^{+/+} males.

SKIP normalizes ASD-linked gene expression in the Adnp^{+/-} mouse brain

In our published gene array analysis in the developing embryo,⁸ a significant difference was seen as a consequence of Adnp haploinsufficiency in Slc9a3r2,²⁰ which is part of the solute carrier family, Slc (a family including > 300 genes). Here, a 2.4 decrease was found in Slc9a3r2 in 5-month-old male Adnp^{+/-} vs Adnp^{+/+} (*P*(FDR) = 0.04). Together with the function enrichment maps (Supplementary Figure 3) indicating a major receptor/transporter involvements, we investigated potential solute carriers associated with ASD, specifically the solute carrier family 6, neurotransmitter transporter, serotonin, member 4 (Slc6a4).⁴⁸ We discovered a

significant increase in male (but not female) of the hippocampal Slc6a4 levels in the Adnp^{+/-}, compared with Adnp^{+/+} mice (*P* < 0.001, Figures 4b and g–i). SKIP treatment reduced Slc6a4 expression levels in the hippocampus of the Adnp^{+/-} mice (*P* < 0.001) to control levels, whereas the control peptide, D-SKIP did not (Figures 4c and g), paving the path to behavioral analysis.

Social recognition test: all male mice prefer a mouse over an object

There was a strong preference of all male mice toward the novel mouse over the object (Figure 5a).¹⁵ In contrast, Adnp^{+/-} females spent significantly less time sniffing the mouse compared with Adnp^{+/+} males, and did not show a significant preference to mice vs objects. SKIP treatment did not affect the overall preference toward the male mouse rather than object, but it significantly decreased the time spent with the object (blue, #*P* < 0.05), which was not affected by the control peptide D-SKIP (blue bars).

Adnp^{+/-} mice social memory impairments are completely reversed by SKIP

The Adnp^{+/-} mice exhibited an abnormal social memory response because, unlike Adnp^{+/+} mice, they did not show renewed interest with the introduction of an unfamiliar mouse and preferred the familiar mouse (Figure 5b).¹⁵ SKIP treatment normalized social

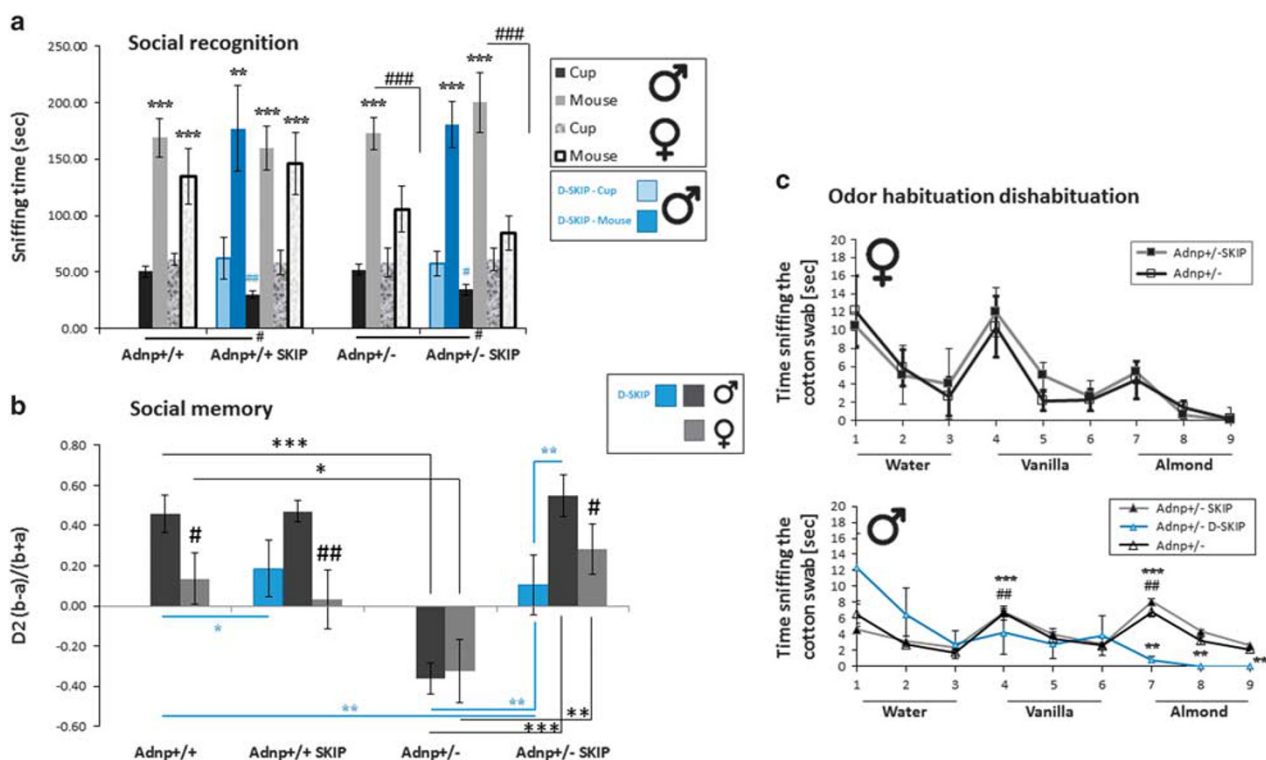


Figure 5. Social and memory differences between males and females, influence of the *Adnp* genotype and improvement by SKIP treatment. **(a)** Social recognition test: unlike males, females do not prefer mouse over object and SKIP treatment does not affect mouse-object preference. Data are expressed as mean (\pm s.e.m.) total time (s) spent exploring mice or objects. An empty wire cup was placed in the center of the right or left chamber as the novel object and the cup containing the target mouse was placed in the center of the other chamber. Location of the novel object and the novel mouse were counterbalanced to avoid confounding effects of side preference. Three-way analysis of variance (ANOVA) revealed no main effect for group ($F(3,199) = 0.118, P = 0.949$) on the sniffing times of a novel mouse and a cup in phase III of the experiment. However, a main effect was found for the sniffed item ($F(1,199) = 135.221, P < 0.001$), indicating a strong preference for the novel mouse over the pencil cup. In addition, a main effect for gender was found ($F(1,199) = 4.594, P = 0.033$). Fisher's LSD *post hoc* test revealed significant differences between sniffing time of the cup and mouse in all male groups and in the *Adnp*^{+/-} females ($***P < 0.001$ vs cup). Fisher's LSD *post hoc* test showed that *Adnp*^{+/-} females spent significantly less time sniffing the mouse compared with *Adnp*^{+/+} males ($###P < 0.001$). For D-SKIP-treated male mice, two-way repeated measures ANOVA revealed main effect for the sniffed item ($F(1,187) = 151.468, P < 0.001$), indicating a strong preference for the novel mouse over the pencil cup. Fisher's LSD *post hoc* test revealed significant differences between sniffing time of the cup and mouse in the male groups ($**P < 0.01, ***P < 0.001$ vs cup). A significant reduction in the sniffing time of the object was observed after SKIP treatment ($^{\#}P < 0.05$), whereas D-SKIP was inert. **(b)** *Adnp*^{+/-} male and female mice display a significantly decreased social memory, SKIP protects. Animal performance in the social memory test is shown (3 h after the original 3 min exposure). Data are expressed as mean (\pm s.e.m.) total time (s) spent exploring other mice designated by relative discrimination index ($b =$ time sniffing a novel mouse, $a =$ time sniffing a familiar mouse). The total time allowed for sniffing in the second exposure was 3 min). Here, the *Adnp*^{+/-} male and female mice spent significantly less time exploring the novel mouse as compared with *Adnp*^{+/+} mice). Three-way ANOVA showed a significant genotype effect ($F(1,96) = 9.333, P = 0.003$) in the social memory test (*Adnp*^{+/+} vs *Adnp*^{+/-} mice), a significant general gender effect (males vs females; $F(1,96) = 10.331, P = 0.002$) and a significant treatment effect ($F(1,96) = 21.316, P < 0.001$). Fisher's LSD *post hoc* test revealed a significant genotype difference between the *Adnp*^{+/+} and *Adnp*^{+/-} in both male and female groups ($***P < 0.001, *P < 0.05$); there was also a significant gender effect in the *Adnp*^{+/+}, *Adnp*^{+/+} SKIP and *Adnp*^{+/-} SKIP groups ($^{\#}P < 0.05, ###P < 0.01$ male vs female). Fisher's LSD *post hoc* test also revealed a significant treatment difference between the *Adnp*^{+/-} and *Adnp*^{+/-} SKIP in both male and female groups ($***P < 0.001$) and in the female group ($**P = 0.002$). For D-SKIP-treated male mice, two-way ANOVA showed a main significant genotype effect ($F(1,91) = 12.565, P < 0.001$), as well as significant main treatment ($F(2,91) = 13.417, P < 0.001$) and interaction ($F(2,91) = 16.324, P < 0.001$) effects. Fisher's LSD *post hoc* test revealed a significant treatment difference between the *Adnp*^{+/+} and *Adnp*^{+/+} D-SKIP ($*P < 0.05$). D-SKIP-treated mice were significantly different from vehicle-treated mice and from SKIP-treated mice ($**P < 0.01$). **(c)** SKIP does not affect olfactory function. Odors were presented on a suspended cotton swab to the test mouse placed into the clean cage with fresh shavings. Each mouse was tested during three consecutive 2-min periods for each odor, with 2-min intervals between presentations. The x axis indicates the consecutive number of the odor exposure period. The time that the mouse smelled the swab was recorded (beginning whenever the animal oriented its nostrils toward the cotton swab, within 2 cm or less). Male: $n = 16-18$. Female: $n = 11$. $^{\#}P < 0.01$ vs previous sniffing (novel vs familiar odor), paired *t*-test. No significant main effects between groups. In contrast, D-SKIP treatment, *Adnp*^{+/-} males; $n = 4$, abolished olfactory discrimination.

memory of the *Adnp*^{+/-} male and female mice (Figure 5b). Generally, *Adnp*^{+/+} females and SKIP-treated *Adnp*^{+/-} females were significantly less interested in the novel over the familiar females compared with the corresponding male interest in novel males. D-SKIP treatment of *Adnp*^{+/-} males resulted in indifference to the novel vs familiar mice, contrasting SKIP-treated mice.

As olfactory cues are the predominant mechanism through which social familiarity develops,⁴⁰ we investigated SKIP effects on odor discrimination. Complete identity was observed between the outbred *Adnp*^{+/-} and *Adnp*^{+/+} genotypes within the same sex¹⁵ and no effect of SKIP treatment (Figure 5c). Thus, the differences observed in social memory could be attributed to

emotional/cognitive disturbance dissociated from olfactory memory. D-SKIP abolished olfactory discrimination (Figure 5c) suggesting an antagonistic activity.

DISCUSSION

The current study implicates Adnp replacement therapy as a potential drug target. The EB3 targeting SKIP enhanced the interaction of the NAPVSIQ motif of Adnp with EB3, suggesting augmentation of Adnp MT fortification under compromised situations, such as Adnp haploinsufficiency. Adnp^{+/-} mice exhibited impaired anterograde axonal transport and SKIP significantly ameliorated these deficiencies. Our results corroborate findings in mice³⁸ and in flies⁴⁹ in which NAP preserved MT-dependent axonal transport. This is relevant as SKIP is a four-amino acid peptide based on the NAP core sequence and peptide shortening by 50% did not result in loss of function. We revealed sexual dichotomy in MT activity (axonal transport). As MTs are key structural proteins in the brain,⁵⁰ this finding is of fundamental importance. Using RNA-seq, we have discovered a significant age/sex effect on specific tubulin isotype expression complementing our original findings of changes of tubulin microheterogeneity with brain development⁵⁰ neurite enriched beta tubulin at the single neuron level⁵¹ and beta tubulin mutations disrupting axonal transport.⁵²

At the behavioral level, 7-month-old Adnp^{+/-} male mice exhibited social memory impairments, while preserving olfactory functions. Two daily treatments with SKIP (for 3 months), significantly ameliorated social memory deficits in the Adnp^{+/-} mice. Social memory is dependent on intact olfaction both in humans⁵³ and animals. As ICR outbred Adnp^{+/-} mice showed intact odor habituation–dishabituation,¹⁵ the deficits in social memory are attributed to emotional/cognitive disturbance dissociated from olfactory memory. Notably, our colony, outbred with ICR mice, is still showing significant behavioral effects in the Adnp^{+/-} mice, which implicates a strong Adnp genotype effect, as predicted from human mutations mimicking the human ADNP haploinsufficient case.⁴⁶ Furthermore, the SKIP effect was not mimicked by D-SKIP, which inhibited olfactory functions. Future studies are planned to further characterize D-SKIP as a potential antagonist.

Most significant genotype-associated changes, which were opposite to each other in males were the reduced hippocampal cells expressing VDCC (Cacnb1) and the increased number of hippocampal cells expressing Slc6a4, both completely reversed to control levels by SKIP treatment. Defects in Ca²⁺ signaling affect synaptogenesis in addition to dendritic arborization, cell survival and gene expression. It was suggested that defects in synaptogenesis are strongly correlated with ASDs⁵⁴ and that some ASDs result from a failure in Ca²⁺-dependent development of the central nervous system.⁵⁵ Importantly, we found sex-dependent difference in hippocampal VDCC expression, which was corroborated by RNA-seq results.

The serotonin transporter, Slc6a4, has been shown to increase in autism.^{56,57} Serotonin is reported to influence neurogenesis and/or neuronal removal, neuronal differentiation and synaptogenesis.⁵⁸ As such, serotonin holds an important role in dendritic development, including overall dendritic length, spine formation and branching in both hippocampus and cortex.⁵⁸ Early disturbance of the serotonergic system disrupts the developmental process and contributes to the neuropathological changes in autism. The genetics background of ASD involves the interplay of > 100 genes, with *de novo* loss-of-function in > 5% of the cases.⁵⁹ Additional estimations involve > 250 genes with > 26 mouse models, showing over and under connectivity, with Slc6a4 playing a major role.⁶⁰ Furthermore, the serotonin-N-acetylserotonin-melatonin pathway was suggested as a major biomarker for ASD⁶¹ and Slc6a4 regulates serotonin expression in a

sex-dependent manner.⁶² Here, the amelioration of Slc6a4 expression was apparent only in the case of SKIP and not D-SKIP treatment, suggesting specificity and association with the behavioral outcome.

The sex-dependent differences in BECN1 expression are in agreement with Ambra1 association with ASD in female mice only¹⁸ and with BECN1 association with the MT system,⁶³ which we are now showing as sexually controlled.

Additional genes of note are shown in Supplementary Figure 4 (Gfap) and Supplementary Table 3. These should be further studied in the context of symptoms found in ADNP-mutated children, including, but not limited to, brain development deficits, auditory, heart, eating and sleep management problems, linked to some of the genes showing major differences among the various conditions studied here and also affected in the ADNP-mutated children.^{3,45,64} However, the two major limitations of this study encompass distinct patterns of human and rodent brain-expressed genes⁶⁵ and the paucity of the molecular knowledge on differences in human brain development compared with rodents.

Our study adds significant new information on the functional alterations in the Adnp^{+/-} mice that can be identified using MEMRI analysis. Adnp^{+/-} mice mimic behavioral and biochemical features of ASD and a connection between the Adnp genotype and ASD genes. Based on the MT EB protein association of Adnp,¹⁹ we identified and characterized a potentially new prototype drug candidate for further studies. SKIP demonstrated similar neuroprotective effects to NAP, with sex-dependent effects, paving the path to potential sex-dependent drug development.⁶⁶ These results have to be taken cautiously, with previous experience in peptide-based drug candidates.⁶⁷ However, genotype, age and sex differences discovered here by RNA-seq analyses, immunohistochemistry and MEMRI highlight MT/ion transporters/serotonin signaling as potential future treatment targets. With cognitive impairment in ASD/Alzheimer's disease/schizophrenia being an unmet tremendous burden on patients, families and the society, these findings are of utmost, general significance.

CONFLICT OF INTEREST

SKIP is under patent protection and under term sheet agreement to Coronis Partners (IG conflict of interest).

ACKNOWLEDGMENTS

Illana Gozes laboratory is supported by the AMN Foundation, the Israel Ministry of Science, Technology and Space, Israel Science Foundation, CFTAU Montreal Circle of Friends and the Adams family, Adams Super Center for Brain Studies, the Edersheim Levie-Gitter Institute for Functional Brain Imaging, the Diana and Zelman Elton (Elbaum) Laboratory for Molecular Neuroendocrinology and the Lily and Avraham Gildor Chair for the Investigation of Growth Factors at Tel Aviv University. Illana Gozes is a Humboldt Award Recipient and was a fellow at the Hanse-Wissenschaftskolleg, Germany. This study is in partial fulfillment graduate studies requirements for Noy Amram, Gal Hacoheh Kleiman, Anna Malishkevich, Jeny Katz and Shlomo Sragovich at the Miriam and Sheldon G. Adelson Graduate School of Medicine, Sackler Faculty of Medicine, Tel Aviv University. We thank Orly Yaron, Genome Center Laboratory, Limor Frish, NMR Laboratory, and Yael Piontkewitz, Alfredo Federico Strauss Center for Computational Neuroimaging at Tel Aviv University and the Technion's Genomic Center for their input and excellent work. We thank Oxana Kapitansky for her help.

REFERENCES

- 1 Gillberg C, Wing L. Autism: not an extremely rare disorder. *Acta Psychiatr Scand* 1999; **99**: 399–406.
- 2 Abrahams BS, Geschwind DH. Advances in autism genetics: on the threshold of a new neurobiology. *Nat Rev Genet* 2008; **9**: 341–355.

- 3 Helsmoortel C, Vulto-van Silfhout AT, Coe BP, Vandeweyer G, Rooms L, van den Ende J *et al*. A SWI/SNF-related autism syndrome caused by de novo mutations in ADNP. *Nat Genet* 2014; **46**: 380–384.
- 4 Zamostiano R, Pinhasov A, Gelber E, Steingart RA, Seroussi E, Giladi E *et al*. Cloning and characterization of the human activity-dependent neuroprotective protein. *J Biol Chem* 2001; **276**: 708–714.
- 5 Borozdin W, Graham JM Jr, Bohm D, Bamshad MJ, Spranger S, Burke L *et al*. Multigene deletions on chromosome 20q13.13-q13.2 including SALL4 result in an expanded phenotype of Okihiro syndrome plus developmental delay. *Hum Mutat* 2007; **28**: 830.
- 6 Bassan M, Zamostiano R, Davidson A, Pinhasov A, Giladi E, Perl O *et al*. Complete sequence of a novel protein containing a femtomolar-activity-dependent neuroprotective peptide. *J Neurochem* 1999; **72**: 1283–1293.
- 7 Pinhasov A, Mandel S, Torchinsky A, Giladi E, Pittel Z, Goldsweig AM *et al*. Activity-dependent neuroprotective protein: a novel gene essential for brain formation. *Brain Res Dev Brain Res* 2003; **144**: 83–90.
- 8 Mandel S, Rechavi G, Gozes I. Activity-dependent neuroprotective protein (ADNP) differentially interacts with chromatin to regulate genes essential for embryogenesis. *Dev Biol* 2007; **303**: 814–824.
- 9 Mandel S, Gozes I. Activity-dependent neuroprotective protein constitutes a novel element in the SWI/SNF chromatin remodeling complex. *J Biol Chem* 2007; **282**: 34448–34456.
- 10 Dresner E, Malishkevich A, Arviv C, Leibman Barak S, Alon S, Ofir R *et al*. Novel evolutionary-conserved role for the activity-dependent neuroprotective protein (ADNP) family that is important for erythropoiesis. *J Biol Chem* 2012; **287**: 40173–40185.
- 11 Schirer Y, Malishkevich A, Ophir Y, Lewis J, Giladi E, Gozes I. Novel marker for the onset of frontotemporal dementia: early increase in activity-dependent neuroprotective protein (ADNP) in the face of Tau mutation. *PLoS One* 2014; **9**: e87383.
- 12 Ewers M, Walsh C, Trojanowski JQ, Shaw LM, Petersen RC, Jack CR Jr *et al*. Prediction of conversion from mild cognitive impairment to Alzheimer's disease dementia based upon biomarkers and neuropsychological test performance. *Neurobiol Aging* 2010; **33**: 1203–1214.
- 13 Luo M, Shen D, Zhou X, Chen X, Wang W. MicroRNA-497 is a potential prognostic marker in human cervical cancer and functions as a tumor suppressor by targeting the insulin-like growth factor 1 receptor. *Surgery* 2013; **153**: 836–847.
- 14 Gozes I, Yeheskel A, Pasmanik-Chor M. Activity-dependent neuroprotective protein (ADNP): a case study for highly conserved chordata-specific genes shaping the brain and mutated in cancer. *J Alzheimers Dis* 2014; **45**: 57–73.
- 15 Malishkevich A, Amram N, Hacohen-Kleiman G, Magen I, Giladi E, Gozes I. Activity-dependent neuroprotective protein (ADNP) exhibits striking sexual dichotomy impacting on autistic and Alzheimer's pathologies. *Transl Psychiatry* 2015; **5**: e501.
- 16 Gkogkas CG, Khoutorsky A, Ran I, Rampakakis E, Nevarko T, Weatherill DB *et al*. Autism-related deficits via dysregulated eIF4E-dependent translational control. *Nature* 2013; **493**: 371–377.
- 17 Merenlender-Wagner A, Malishkevich A, Shemer Z, Udawela M, Gibbons A, Scarr E *et al*. Autophagy has a key role in the pathophysiology of schizophrenia. *Mol Psychiatry* 2015; **20**: 126–132.
- 18 Dere E, Dahm L, Lu D, Hammerschmidt K, Ju A, Tantra M *et al*. Heterozygous *ambra1* deficiency in mice: a genetic trait with autism-like behavior restricted to the female gender. *Front Behav Neurosci* 2014; **8**: 181.
- 19 Oz S, Kapitansky O, Ivashco-Pachima Y, Malishkevich A, Giladi E, Skalka N *et al*. The NAP motif of activity-dependent neuroprotective protein (ADNP) regulates dendritic spines through microtubule end binding proteins. *Mol Psychiatry* 2014; **19**: 1115–1124.
- 20 Vulih-Shultzman I, Pinhasov A, Mandel S, Grigoriadis N, Touloumi O, Pittel Z *et al*. Activity-dependent neuroprotective protein snippet NAP reduces tau hyperphosphorylation and enhances learning in a novel transgenic mouse model. *J Pharmacol Exp Ther* 2007; **323**: 438–449.
- 21 Gozes I, Morimoto BH, Tiong J, Fox A, Sutherland K, Dangoor D *et al*. NAP: research and development of a peptide derived from activity-dependent neuroprotective protein (ADNP). *CNS Drug Rev* 2005; **11**: 353–368.
- 22 Gozes I. Tau pathology: predictive diagnostics, targeted preventive and personalized medicine and application of advanced research in medical practice. *EPMA J* 2010; **1**: 305–316.
- 23 Morimoto BH, Schmechel D, Hirman J, Blackwell A, Keith J, Gold M. A double-blind, placebo-controlled, ascending-dose, randomized study to evaluate the safety, tolerability and effects on cognition of AL-108 after 12 weeks of intranasal administration in subjects with mild cognitive impairment. *Dement Geriatr Cogn Disord* 2013; **35**: 325–336.
- 24 Magen I, Gozes I. Microtubule-stabilizing peptides and small molecules protecting axonal transport and brain function: focus on davunetide (NAP). *Neuropeptides* 2013; **47**: 489–495.
- 25 Jarskog LF, Dong Z, Kangarlou A, Colibazzi T, Giris RR, Kegeles LS *et al*. Effects of davunetide on N-acetylaspartate and choline in dorsolateral prefrontal cortex in patients with schizophrenia. *Neuropsychopharmacology* 2013; **38**: 1245–1252.
- 26 Javitt DC, Buchanan RW, Keefe RS, Kern R, McMahon RP, Green MF *et al*. Effect of the neuroprotective peptide davunetide (AL-108) on cognition and functional capacity in schizophrenia. *Schizophr Res* 2012; **136**: 25–31.
- 27 Simmons A, Westman E, Muehlboeck S, Mecocci P, Vellas B, Tsolaki M *et al*. The AddNeuroMed framework for multi-centre MRI assessment of Alzheimer's disease: experience from the first 24 months. *Int J Geriatr Psychiatry* 2011; **26**: 75–82.
- 28 Divinski I, Mittelman L, Gozes I. A femtomolar acting octapeptide interacts with tubulin and protects astrocytes against zinc intoxication. *J Biol Chem* 2004; **279**: 28531–28538.
- 29 Ewers M, Cheng X, Nural HF, Walsh C, Meindl T, Teipel SJ *et al*. Increased CSF-BACE1 activity associated with decreased hippocampus volume in Alzheimer's disease. *J Alzheimers Dis* 2010; **25**: 373–381.
- 30 Breneman DE, Hauser J, Neale E, Rubinraut S, Fridkin M, Davidson A *et al*. Activity-dependent neurotrophic factor: structure-activity relationships of femtomolar-acting peptides. *J Pharmacol Exp Ther* 1998; **285**: 619–627.
- 31 Wilkemeyer MF, Chen SY, Menkari CE, Breneman DE, Sulik KK, Charness ME. Differential effects of ethanol antagonism and neuroprotection in peptide fragment NAPVSIQP prevention of ethanol-induced developmental toxicity. *Proc Natl Acad Sci USA* 2003; **100**: 8543–8548.
- 32 Sun H. A universal molecular descriptor system for prediction of logP, logS, logBB, and absorption. *J Chem Inf Comput Sci* 2004; **44**: 748–757.
- 33 Honnappa S, Gouveia SM, Weisbrich A, Damberger FF, Bhavesh NS, Jawhari H *et al*. An EB1-binding motif acts as a microtubule tip localization signal. *Cell* 2009; **138**: 366–376.
- 34 Bjelic S, De Groot CO, Scharer MA, Jaussi R, Bargsten K, Salzmann M *et al*. Interaction of mammalian end binding proteins with CAP-Gly domains of CLIP-170 and p150(glued). *J Struct Biol* 2012; **177**: 160–167.
- 35 Raveh B, London N, Schueler-Furman O. Sub-angstrom modeling of complexes between flexible peptides and globular proteins. *Proteins* 2010; **78**: 2029–2040.
- 36 Dangoor D, Biondi B, Gobbo M, Vachutinski Y, Fridkin M, Gozes I *et al*. Novel glycosylated VIP analogs: synthesis, biological activity, and metabolic stability. *J Pept Sci* 2008; **14**: 321–328.
- 37 Alcalay RN, Giladi E, Pick CG, Gozes I. Intranasal administration of NAP, a neuroprotective peptide, decreases anxiety-like behavior in aging mice in the elevated plus maze. *Neurosci Lett* 2004; **361**: 128–131.
- 38 Batool F, Hasnat A, Haleem MA, Haleem DJ. Dose-related effects of clozapine and risperidone on the pattern of brain regional serotonin and dopamine metabolism and on tests related to extrapyramidal functions in rats. *Acta Pharm* 2010; **60**: 129–140.
- 39 McFarlane HG, Kusek GK, Yang M, Phoenix JL, Bolivar VJ, Crawley JN. Autism-like behavioral phenotypes in BTBR T+tf/J mice. *Genes Brain Behav* 2008; **7**: 152–163.
- 40 El-Kordi A, Winkler D, Hammerschmidt K, Kastner A, Krueger R, Ronnenberg A *et al*. Development of an autism severity score for mice using Nlgn4 null mutants as a construct-valid model of heritable monogenic autism. *Behav Brain Res* 2013; **251**: 41–49.
- 41 Matsuoka Y, Jouroukhin Y, Gray AJ, Ma L, Hirata-Fukae C, Li HF *et al*. A neuronal microtubule-interacting agent, NAPVSIQP, reduces tau pathology and enhances cognitive function in a mouse model of Alzheimer's disease. *J Pharmacol Exp Ther* 2008; **325**: 146–153.
- 42 Gregg B, Thiessen DD. A simple method of olfactory discrimination of urines for the Mongolian gerbil, *Meriones unguiculatus*. *Physiol Behav* 1981; **26**: 1133–1136.
- 43 Heckemann RA, Keihaninejad S, Aljabar P, Gray KR, Nielsen C, Rueckert D *et al*. Automatic morphometry in Alzheimer's disease and mild cognitive impairment. *Neuroimage* 2011; **56**: 2024–2037.
- 44 Vaisburd S, Shemer Z, Yeheskel A, Giladi E, Gozes I. Risperidone and NAP protect cognition and normalize gene expression in a schizophrenia mouse model. *Sci Rep* 2015; **5**: 16300.
- 45 Gozes I, Helsmoortel C, Vandeweyer G, Van der Aa N, Kooy F, Sermone SB. The compassionate side of neuroscience: Tony Sermone's Undiagnosed genetic journey—ADNP mutation. *J Mol Neurosci* 2015; **56**: 751–757.
- 46 Vandeweyer G, Helsmoortel C, Van Dijk A, Vulto-van Silfhout AT, Coe BP, Bernier R *et al*. The transcriptional regulator ADNP links the BAF (SWI/SNF) complexes with autism. *Am J Med Genet C Semin Med Genet* 2014; **166C**: 315–326.
- 47 Hakim F, Wang Y, Carreras A, Hirotsu C, Zhang J, Peris E *et al*. Chronic sleep fragmentation during the sleep period induces hypothalamic endoplasmic reticulum stress and PTP1b-mediated leptin resistance in male mice. *Sleep* 2015; **38**: 31–40.
- 48 Murphy DL, Fox MA, Timpano KR, Moya PR, Ren-Patterson R, Andrews AM *et al*. How the serotonin story is being rewritten by new gene-based discoveries principally related to SLC6A4, the serotonin transporter gene, which functions to influence all cellular serotonin systems. *Neuropharmacology* 2008; **55**: 932–960.
- 49 Quraishi S, Cowan CM, Mudher A. NAP (davunetide) rescues neuronal dysfunction in a Drosophila model of tauopathy. *Mol Psychiatry* 2013; **18**: 834–842.
- 50 Gozes I, Littauer UZ. Tubulin microheterogeneity increases with rat brain maturation. *Nature* 1978; **276**: 411–413.

- 51 Gozes I, Sweadner KJ. Multiple tubulin forms are expressed by a single neurone. *Nature* 1981; **294**: 477–480.
- 52 Nakamachi T, Ohtaki H, Yofu S, Dohi K, Watanabe J, Hayashi D *et al*. Pituitary adenylate cyclase-activating polypeptide (PACAP) type 1 receptor (PAC1R) co-localizes with activity-dependent neuroprotective protein (ADNP) in the mouse brains. *Regul Pept* 2008; **145**: 88–95.
- 53 Li W, Moallem I, Paller KA, Gottfried JA. Subliminal smells can guide social preferences. *Psychol Sci* 2007; **18**: 1044–1049.
- 54 Chih B, Afridi SK, Clark L, Scheiffele P. Disorder-associated mutations lead to functional inactivation of neuroligins. *Hum Mol Genet* 2004; **13**: 1471–1477.
- 55 Krey JF, Dolmetsch RE. Molecular mechanisms of autism: a possible role for Ca²⁺ signaling. *Curr Opin Neurobiol* 2007; **17**: 112–119.
- 56 Laurence JA, Fatemi SH. Glial fibrillary acidic protein is elevated in superior frontal, parietal and cerebellar cortices of autistic subjects. *Cerebellum* 2005; **4**: 206–210.
- 57 Mulder EJ, Anderson GM, Kema IP, de Bildt A, van Lang ND, den Boer JA *et al*. Platelet serotonin levels in pervasive developmental disorders and mental retardation: diagnostic group differences, within-group distribution, and behavioral correlates. *J Am Acad Child Adolesc Psychiatry* 2004; **43**: 491–499.
- 58 Whitaker-Azmitia PM. Serotonin and brain development: role in human developmental diseases. *Brain Res Bull* 2001; **56**: 479–485.
- 59 De Rubeis S, He X, Goldberg AP, Poultney CS, Samocha K, Cicek AE *et al*. Synaptic, transcriptional and chromatin genes disrupted in autism. *Nature* 2014; **515**: 209–215.
- 60 Ellegood J, Anagnostou E, Babineau BA, Crawley JN, Lin L, Genestine M *et al*. Clustering autism: using neuroanatomical differences in 26 mouse models to gain insight into the heterogeneity. *Mol Psychiatry* 2015; **20**: 118–125.
- 61 Pagan C, Delorme R, Callebort J, Goubran-Botros H, Amsellem F, Drouot X *et al*. The serotonin-N-acetylserotonin-melatonin pathway as a biomarker for autism spectrum disorders. *Transl Psychiatry* 2014; **4**: e479.
- 62 Jazin E, Cahill L. Sex differences in molecular neuroscience: from fruit flies to humans. *Nat Rev Neurosci* 2010; **11**: 9–17.
- 63 Luo S, Garcia-Arencibia M, Zhao R, Puri C, Toh PP, Sadiq O *et al*. Bim inhibits autophagy by recruiting Beclin 1 to microtubules. *Mol Cell* 2012; **47**: 359–370.
- 64 Pescosolido MF, Schwede M, Johnson Harrison A, Schmidt M, Gamsiz ED, Chen WS *et al*. Expansion of the clinical phenotype associated with mutations in activity-dependent neuroprotective protein. *J Med Genet* 2014; **51**: 587–589.
- 65 Ponting CP, Goodstadt L. Separating derived from ancestral features of mouse and human genomes. *Biochem Soc Trans* 2009; **37**: 734–739.
- 66 Cahill L. A half-truth is a whole lie: on the necessity of investigating sex influences on the brain. *Endocrinology* 2012; **153**: 2541–2543.
- 67 Nissen KB, Andersen JJ, Haugaard-Kedstrom LM, Bach A, Stromgaard K. Design, synthesis, and characterization of fatty acid derivatives of a dimeric peptide-based postsynaptic density-95 (PSD-95) inhibitor. *J Med Chem* 2015; **58**: 1575–1580.

Supplementary Information accompanies the paper on the Molecular Psychiatry website (<http://www.nature.com/mp>)